Thermal stability and frequency up-conversion properties of Er^{3+}-doped oxyfluoride tellurite glasses

Dongbing He (何冬兵), Junjie Zhang (张军杰), Guonian Wang (汪国年), Zhongchao Duan (段忠超), Shixun Dai (戴世勋), and Lili Hu (胡丽丽)

Shanghai Institute of Optics and Fine Mechanics, Chinese Academy of Sciences, Shanghai 201800

Received April 11, 2005

The thermal properties of $68TeO_2$-$15BaF_2$-$5SrF_2$-$10LaF_3$-2KF glass were measured by different temperature analysis (DTA). Up-conversion luminescence of Er^{3+} ion in the obtained glass was investigated. Mechanism of up-conversion emission was discussed. The result shows that the obtained oxyfluoride tellurite glass $68TeO_2$-$15BaF_2$-$5SrF_2$-$10LaF_3$-2KF has a good thermal stability (ΔT = 153.6 °C) and strong up-conversion green emissions around 527 nm and 549 nm and red emission at 660 nm. This glass can be a promising host material for up-conversion fiber lasers.

OCIS codes: 160.5690, 160.4670, 300.6280, 160.2750, 160.2540.

In recent years, there have been continuous efforts to the development of rare-earth doped up-conversion lasers. Some of their many applications include infrared pumped ultraviolet (UV)-visible lasers, color displays, high density optical date reading/storage, biomedical diagnostics, infrared laser viewers, and indicators[1].

Infrared or red radiation induced up-conversion processes have been widely observed in fluoride glasses doped with different rare-earth ions due to their lower phonon energy[2]. However, its poor chemical durability, low mechanical strength, and low glass transition temperature have caused serious problems for its practical applications.

In general, it is difficult to generate up-conversion in conventional oxide glasses due to their high phonon energies (> 1000 cm^{-1}), corresponding to the stretching vibrations of the oxide glasses network former. Though up-conversion fluorescence has been reported in Er^{3+}-doped tellurite glasses[3,4], due to their relatively low phonon energy (800 cm^{-1}), their emission intensity, quantum efficiency, and thermal stability show that tellurite glasses are not desirable for up-conversion lasers.

A series of further studies show that oxyfluoride tellurite glass is a good host material, which not only has relative low phonon energy between tellurite glasses and fluoride glasses but also has good thermal stability, chemical durability and mechanical strength[5,6]. The oxyfluoride tellurite glass is then thought as a promising host material for optical applications such as fiber lasers and fiber amplifiers. Some oxyfluoride tellurite glasses[5−7] have been obtained and investigated, which show an increase in optical property. In this work, we have obtained an oxyfluoride tellurite glasses, which has good thermal stability (ΔT = 153.6 °C) and optical performance.

Starting materials (except ErF_3) with high purity of about 99.997% were mixed. The ErF_3 with purity of 99.9% was last mixed in 1 wt.-%. Mixed bathe was melted in platinum crucibles at 900—1000 °C for 30 minutes while being bubbled with dry air, then the liquids were poured into graphite molds preheated near their glass transition temperature in 1 hour. After annealing for 20 hours, samples were cut and polished to the size of 20 × 10 × 2 (mm) for optical property measurements.

The glasses transition, crystallization-onset and peak crystallization temperatures were measured by different thermal analysis (DTA). The DTA was performed with a NETZSCH STA 409 PC/PG apparatus under Ar atmosphere at a heating rate of 10 $K \cdot min^{-1}$.

The index of refraction was measured at 656.3 nm, with a precision V-prism refractometer using H_2 and Na lamps as spectral sources.

The absorption spectra were measured using a Perkin-Elmer900 spectrophotometer in the range of 300—1700 nm at room temperature. The up-conversion luminescence spectrum was obtained with a TRIAX550 spectrofluorimeter upon excitation of 980-nm laser diode (LD) with a maximum power of 2 W. All the measurements were taken at the room temperature.

Figure 1 shows the DTA curves of $68TeO_2$-$15BaF_2$-$5SrF_2$-$10LaF_3$-2 KF glasses. The glasses transition temperature T_g was 403.1 °C, crystallization-onset temperature T_X was 556.7 °C, and melting-onset temperature T_c was 571.4 °C. In general, the parameter ΔT ($T_X - T_g$) was used to simply evaluate the thermal stability of the glass against crystallization, ΔT represents the temperature interval during the nucleation taking

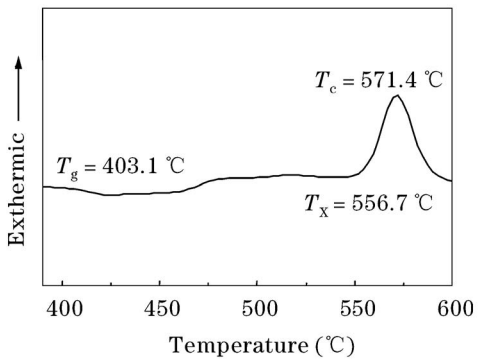

Fig. 1. DTA patterns of oxyfluoride tellurite glasses $68TeO_2$-$15BaF_2$-$5SrF_2$-$10LaF_3$-2KF. T_c is the peak crystallization temperature.

Table 1. Characteristic Temperatures of Different Glasses (Unit: °C)

Glass (mol %)	T_g	T_X	ΔT
$89TeO_2$-$11BaO$[8]	325	468	143
$68TeO_2$-$15BaF_2$-$5SrF_2$-$10LaF_3$-2KF	403.1	556.7	153.6
ZBLAN[10]	262	352	90

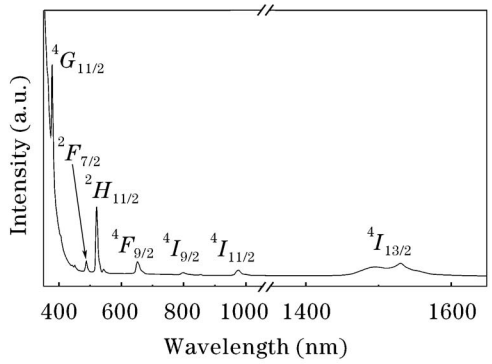

Fig. 2. Absorption spectrum of 1 wt.-% Er^{3+}-doped glass $68TeO_2$-$15BaF_2$-$5SrF_2$-$10LaF_3$-2KF.

place[9]. For drawing of fibers, an index value of ΔT is at least 100 °C, preferably higher than 125 °C. From Table 1, we can find that the obtained glass has a good thermal stability compared with other tellurite glasses and oxyfluoride tellurite glasses. In this glass $68TeO_2$-$15BaF_2$-$5SrF_2$-$10LaF_3$-2KF, the ΔT can reach 153.6 °C, which is desirable for fiber components.

Figure 2 shows the absorption spectrum of erbium ion in the $68TeO_2$-$15BaF_2$-$5SrF_2$-$10LaF_3$-2KF glass in the spectral range from 350 to 1700 nm at the room temperature. All relevant internal $4f$-$4f$ electronic transitions of Er^{3+} ions in the range of 370—1700 nm have been identified. The Judd-Ofelt parameters Ω_2, Ω_4, Ω_6 of the glass were calculated according to the absorption spectrum of the glass. The Ω_2 parameter is sensitive to the symmetry of the rare-earth site and the covalency between rare-earth ions and ligand anions[11]. The rigidity of the network surrounding the rare-earth ion was suggested to influence the magnitude of Ω_4 and Ω_6[12]. From Table 2, the sum Judd-Ofelt parameter is in accordance with reported result which predicted that the sum of the Judd-Ofelt parameter increases in the order fluoride < oxyfluoride < oxide glasses mostly due to the covalency of the chemical bond between the rare-earth ion and the ligand anions[13]. In the obtained glasses, the Ω_2 value was 5.85×10^{-20} cm^{-2}, the Ω_4 value was 1.72×10^{-20} cm^{-2}, and the Ω_6 value was 0.89×10^{-20} cm^{-2}. The decrease of Ω_2 value compared with that in tellurite glasses indicated that the incorporation of fluoride changed the network of original glasses. The

Table 2. Judd-Ofelt Intensity Parameters of Er^{3+}-Doped Different Glasses (Unit: $\times 10^{-20}$ cm^{-2})

Glass	Ω_2	Ω_4	Ω_6
Tellurite[14]	6.98	2.52	1.10
TBSLK	5.85	1.72	0.89
Fluorite[10]	2.91	1.27	1.11

structure of tellurite glasses is mostly made of asymmetrical unit structure of trigonal bipyramids TeO_4 and then Te-$_{ax}$O$_{eq}$-Te linkages as in three-dimensional network of α-TeO_2 crystal[6]. The incorporation of F^- leads to disruption of Te-$_{ax}$O$_{eq}$-Te linkages and then the formation of individual Te-O bonds. The individual Te-O bonds polymerize to Te-O-Te linkages which increase the symmetry of the structure. In addition, the presence of fluoride within the host matrix results in not only the decrease of the global optical basicity of the network but also covalancy between Er^{3+} and the ligand anions[6].

The emission spectrum of Er^{3+} in the visible wavelength range of 500—600 nm under 980-nm excitation at the room temperature is shown in Fig. 3. Two intense green emissions centered at around 527 and 549 nm are clearly observed corresponding to the $^2H_{11/2} \rightarrow {}^4I_{15/2}$ and $^4S_{3/2} \rightarrow {}^4I_{15/2}$ transitions, respectively. In addition, the blue and red emissions are too weak to be observed.

Figure 4 shows the fluorescence up-conversion mechanism of Er^{3+} in the $68TeO_2$-$15BaF_2$-$5SrF_2$-$10LaF_3$-2KF glass. Green emission of Er^{3+} is a two-photon process[15]. Er^{3+} ion is excited initially from the ground state $^4I_{15/2}$ to the $^4I_{11/2}$ state through ground state absorption (GSA) process under 980-nm excitation. The same ion excited to $^4I_{11/2}$ state absorbs a second photon and is then promoted to the state $^4F_{7/2}$. The excited ion then relaxes nonradiatively to the intermediate state of

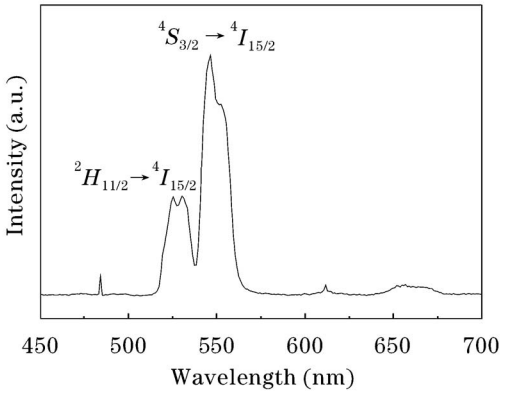

Fig. 3. Up-conversion emission spectrum of Er^{3+} in the glass under 980-nm excitation.

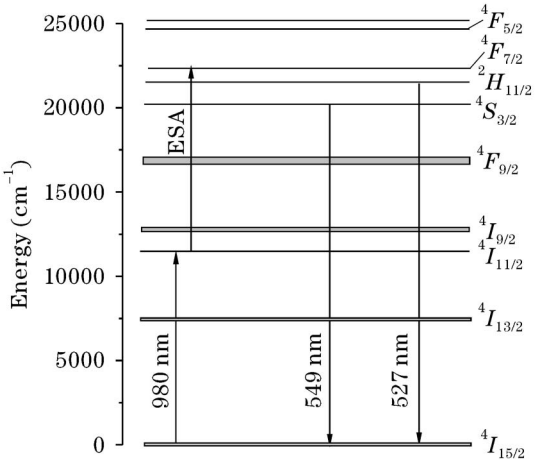

Fig. 4. Up-conversion mechanism of Er^{3+} in glass.

$^2H_{11/2}$ and gives 527-nm green emission through $^2H_{11/2} \rightarrow {}^4I_{15/2}$ process. Er^{3+} ion at the $^4F_{7/2}$ state can also decay to the $^4S_{3/2}$ state due to multiphonon relaxation process (MRP), and gives 549-nm green emission through $^4S_{3/2} \rightarrow {}^4I_{15/2}$ process. The estimated energy gap between the $^2H_{11/2}$ state and the next $^4S_{3/2}$ state is around 800 cm^{-1}, thus multiphonon relaxation rate of $^2H_{11/2} \rightarrow {}^4S_{3/2}$ is very large, so the 527-nm emission intensity is reduced and 549-nm emission intensity is very prominent.

The up-conversion emission of Er^{3+} ions is a two-photon process (or three-photon process), which requires a high pump rate to achieve population inversion. In addition, the low absorption cross section of Er^{3+} ions at 980 nm limits the pump efficiency. Yb^{3+} ions exhibit not only a large absorption cross section but also a broad absorption band between 800 and 1100 nm. Furthermore, the large spectral overlap between Yb^{3+} emission ($^2F_{7/2} \rightarrow {}^2F_{5/2}$) and Er^{3+} absorption ($^4I_{15/2} \rightarrow {}^4I_{13/2}$) results in an efficient resonant energy transfer from Yb^{3+} to Er^{3+} in the Yb^{3+}/Er^{3+} co-doped system. From Fig. 5, we can distinctly see that in the Yb^{3+}/Er^{3+} co-doped system, the intensity of absorption at 980 nm increases greatly. Figure 6 gives the up-conversion emission spectrum of Yb^{3+}/Er^{3+} co-doped oxyfluoride tellurite glass, it can be seen that both the green emissions at 527 and

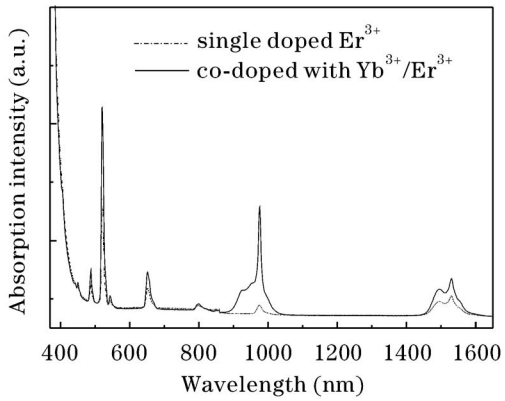

Fig. 5. Absorption spectra of single Er^{3+}-doped glass and co-doped of Yb^{3+}/Er^{3+} (1:1) glass under 980-nm excitation at room temperature.

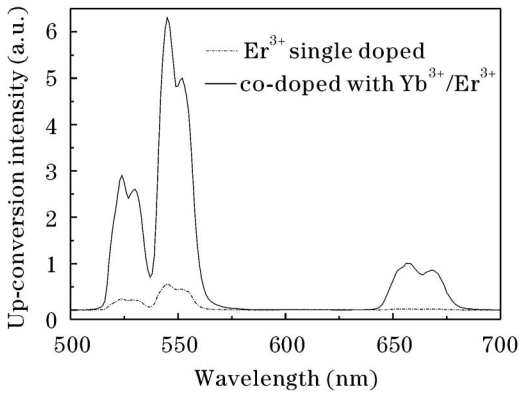

Fig. 6. Up-conversion emission spectra of single doped Er^{3+} and co-doped Yb^{3+}/Er^{3+} (1:1) in the glass under 980-nm excitation.

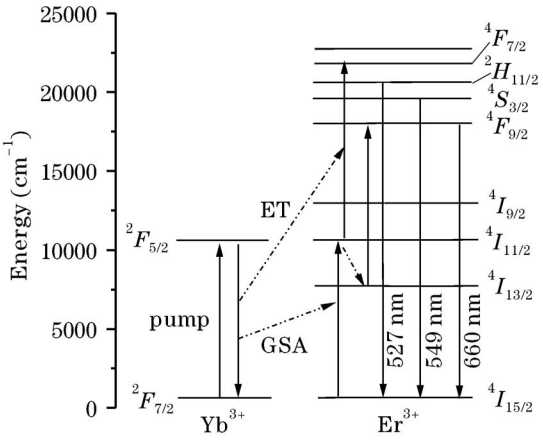

Fig. 7. Simplified energy level diagram of Yb^{3+} and Er^{3+} and possible transition pathways yield under 980-nm excitation.

549 nm and the red emission at 660 nm increase by a factor of 15.

According to the simplified energy levels graph of Yb^{3+} and Er^{3+} illustrated in Fig. 7, the possible up-conversion mechanisms for three emission bands are discussed as follows[16,17]. First, the $^4I_{11/2}$ level of Er^{3+} is directly excited by 980-nm pump and by energy transfer (ET) process from the $^2F_{5/2}$ level of Yb^{3+}: $^2F_{5/2}$ (Yb^{3+}) + $^4I_{15/2}$(Er^{3+}) $\rightarrow {}^2F_{7/2}$(Yb^{3+}) + $^4I_{11/2}$(Er^{3+}). Since Yb^{3+} has a much larger absorption cross section than that of Er^{3+} at 980 nm, the GSA of Er^{3+} from $^4I_{15/2} \rightarrow {}^4I_{11/2}$ is not the main reason for the population of the $^4I_{11/2}$ level of Er^{3+}. The high population accumulation on the $^4I_{11/2}$ level is supposed to serve as the intermediate state responsible for the up-conversion process. Second, some portions of Er^{3+} ions in the $^4I_{11/2}$ level relax rapidly to $^4I_{13/2}$ level through the non-radiative process, consequently. Other portions of Er^{3+} in the $^4I_{11/2}$ level may have two processes, one is ET: $^4I_{11/2}$(Er^{3+}) + $^4I_{11/2}$(Er^{3+}) $\rightarrow {}^4F_{7/2}$(Er^{3+}) + $^4I_{15/2}$(Er^{3+}), and the other the excited state absorption (ESA): $^4I_{11/2}$(Er^{3+}) + a photon $\rightarrow {}^4F_{7/2}$(Er^{3+}). The populated $^4F_{7/2}$ level then relaxes rapidly to the next lower levels $^2H_{11/2}$ and $^4S_{3/2}$ resulting from the small energy gap between them. Third, some populated Er^{3+} ions in the $^2H_{11/2}$ level relax radiatively to the ground level, which produces the green light at 527 nm. Other populated Er^{3+} ions in the $^2H_{11/2}$ level relax to the $^4S_{3/2}$ level through the fast thermal equilibrium process. The populated Er^{3+} ions in the $^4S_{3/2}$ level transit to the ground level and emit green light at 549 nm. The red emission at 660 nm can be contributed to the radiatively transition of the populated Er^{3+} in the $^4S_{3/2}$ level to the ground level. The accumulation of populated Er^{3+} in the $^4S_{3/2}$ level can be obtained by the ESA process: $^4I_{13/2}$(Er^{3+}) + a photon$\rightarrow {}^4F_{9/2}$(Er^{3+}).

In summary, an oxyfluoride tellurite glass $68TeO_2$-$15BaF_2$-$5SrF_2$-$10LaF_3$-2KF with a good thermal stability was obtained, the ΔT ($T_X - T_g$) can reach 153.6 °C. The frequency up-conversion of single doped Er^{3+} and co-doped of Yb^{3+}/Er^{3+} in this glass has been investigated under 980-nm excitation. The green emissions centered

at around 527 and 549 nm were clearly observed both at single doped Er^{3+} and co-doped Yb^{3+}/Er^{3+}, the red emission at 660 nm was only seen in the Yb^{3+}/Er^{3+} co-doped system. This glass with good thermal stability and excellent up-conversion property can be a promising host material for rare-earth doped up-conversion fiber laser system.

This work was financially supported by the Rising-Star Project of Shanghai Municipal Science and Technology Commission (No. 04QMX1448) and the National Natural Science Foundation of China (No. 50572110). D. He's e-mail address is hd6798123@163.com.

References

1. A. S. Gouveia-Neto, E. B. da Costa, L. A. Bueno, and S. J. L. Ribeiro, Opt. Mater. **26,** 271 (2004).
2. M.-F. Joubert, Opt. Mater. **11,** 181 (1999).
3. A. Kanoum, N. Jaba, and A. Brenier, Opt. Mater. **26,** 79 (2004).
4. S. Tanabe, K. Hirao, and N. Soga, J. Non-Cryst. Solids **122,** 79 (1990).
5. V. Nazabal, S. Todoroki, A. Nukui, T. Matsumoto, S. Suohara, T. Hondo, T. Araki, S. Inoue, C. Rivero, and T. Cardinal, J. Non-Cryst. Solids **325,** 85 (2003).
6. V. Nazabal, S. Todoroki, S. Inoue, T. Matsumoto, S. Suehara, T. Hondo, T. Araki, and T. Cardinal, J. Non-Cryst. Solids **326&327,** 359 (2003).
7. S. Xu, H. Ma, D. Fang, Z. Zhang, L. Hu, and Z. Jiang, Chin. Opt. Lett. **3,** 536 (2005).
8. J. S. Wang, E. M. Vogel, and E. Snitzer, Opt. Mater. **3,** 187 (1994).
9. G. S. Murugan and Y. Ohishi, J. Non-Cryst. Solids **341,** 86 (2004).
10. J.-L. Adam, J. Fluor. Chem. **107,** 265 (2001).
11. S. Tanabe, J. Non-Cryst. Solids **259,** 1 (1999).
12. M. J. Weber, J. Non-Cryst. Solids **47,** 117 (1982).
13. P. Nachimuthu and R. Jagannathan, J. Am. Ceram. Soc. **82,** 387 (1999).
14. H. C. Doo, G. C. Yong, and H. K. Kyong, ETRI Journal **23,** 151 (2001).
15. H. Scheife, G. Huber, E. Heumann, S. Bar, and E. Osiac, Opt. Mater. **26,** 365 (2004).
16. V. K. Bogdanov, D. J. Booth, and W. E. K. Gibbs, J. Non-Cryst. Solids **321,** 20 (2003).
17. M. J. F. Digonnet, *Rare-Earth-Doped Fiber Lasers and Amplifiers* (Marcel Dekker, New York, 2001) chap.4.